The Influence of Chemical Mechanisms on PDF Calculations of Nonpremixed Piloted Jet Flames

Renfeng Cao and Stephen B. Pope

Sibley School of Mechanical and Aerospace Engineering, Cornell University, Ithaca, NY 14853, USA

1. Introduction

There are several previous successful PDF modeling studies [1-3] of the Barlow & Frank nonpremixed piloted jet flames (flames D, E and F) [4]. While there is at least partial understanding of the influence of turbulent mixing models on these calculations [5,6], there has been no systematic study of the influence of the chemical mechanism that is employed. In this work, focusing on flame F (which has significant local extinction and exhibits the strongest sensitivity), we present PDF calculations using six different mechanisms. These range from a 5-step reduced mechanism [7], to the GRI3.0 detailed mechanism [8] which involves 53 species. The principal results considered (which are compared to the experimental data [9]) are means of temperature and species mass fraction conditional on mixture fraction. More details of the current work are provided in [10].

2. The joint velocity-turbulence frequency-composition PDF method

There are three different kinds of PDF methods [11]. The simplest one is the composition PDF method, in which only the modelled joint PDF equation for composition is solved: the mean flow field equations are solved by a standard CFD code, and the PDF provides the chemistry closure. The second kind is based on the joint velocity-composition PDF method, in which a separate model is required for the time or length scale of the turbulence. The most complete PDF method is the joint velocity-turbulence frequency-composition PDF method: this is used in the current work and is subsequently referred as the joint PDF method.

The particle implementation of the joint PDF method requires models for mixing, velocity and turbulent frequency following a fluid particle [11]. The SLM (Simplified Langevin Model) is used for the evolution of the particle velocity. The stochastic frequency model of Van Slooten et al. [12] is used for the turbulent frequency of particles, which provides the time scale of turbulence. The model constants used are the same as those used in many previous studies, e.g. [6,13,14].

In PDF methods, the effect of molecular diffusion on the composition is represented by a mixing model. The mixing model constant C_φ is traditionally set to 2.0; but different values have also been used in previous PDF calculations. The EMST [15] mixing model is used in the present work to investigate the effect of different chemical mechanisms. The influence of C_φ is examined by performing calculations with the values C_φ =1.2, 1.5, 2.0 and 3.0 for different chemistry mechanisms.

The chemical mechanisms considered in this paper are listed in Table 1. The GRI detailed kinetic mechanism provides the most comprehensive and standardized set of mechanisms for methane combustion [8]. The detailed versions of 2.11 and 3.0 are investigated and denoted as GRI2.11 and GRI3.0, respectively.

The 15-step reduced GRI2.11 mechanism [16] is denoted by ARM2 following Tang et al. [22]. This mechanism has been successfully used in the joint PDF calculations of flame F performed by Xu, Tang and Pope [1,2]. The 5-step reduced GRI2.11 mechanism[7] is denoted as S5G211 in current paper. The detail description of the skeletal mechanism is provided by James et al. [17]. The Smooke mechanism is described in [18], but three reactions have been updated [19] and are shown in Table 2.

Table 1. Chemical mechanisms used in the present comparisons

Mechanism	# of species	# of steps	NO species	Reference
GRI 2.11	49	277	With NO	[8]
GRI 3.0	53	325	With NO	[8]
ARM2	19	15	With NO	[16]
S5G211	9	5	With NO	[7]
Skeletal	16	41	Without NO	[17]
Smooke	16	46	Without NO	[18,19]

Table 2. Three updates to the Smooke mechanism

REACTIONS	$k = A\,T^b \exp(-E/RT)$		
	A	b	E
$CH_4+H=CH_3+H_2$	2.2×10^4	3.0	8750.
$H+O_2=OH+O$	2.0×10^{14}	0.0	16800.
$H+O_2+M=HO_2+M$	2.1×10^{18}	-1.0	0.
	H_2O/21./ CO_2/5.0/ H_2/3.3/ CO/2.0/ O_2/0.0/ N_2/ 0.0/		

3. Numerical solutions

There are several implementations of particle-mesh methods to solve the modelled joint PDF equations. All computations presented here use a code named HYB2D [14] which implements a hybrid FV/particle algorithm. In the hybrid algorithm, the PDF/particle method (particle part) is coupled with a finite volume solver (FV part). The FV part solves the mean conservation equations for mass,

momentum, energy and the mean equation of state; and the particle part solves the fluctuating velocity-turbulent frequency-compositions PDF transport equations. The FV part provides mean fields of velocity, density and pressure to the particle part and obtains the turbulent fluxes and reaction source term from the particle part.

The flow considered here is statistically steady 2D axisymmetric, and non-swirling. A polar-cylindrical (z,r) coordinate system is used with the origin at the center of the fuel jet at its exit plane. The computational domain is rectangular, of extent (0,80D) in the axial (z) direction, and (0,20D) in the radial (r) direction, where D is the diameter of the jet (D=3.6mm).

The inlet velocity profile is interpolated from measurements [9,20]. The ratio of production to dissipation of turbulent kinetic energy is specified as unity which, together with the specified profiles, determines the inlet profile of mean turbulence frequency. The temperature, compositions, and density are specified as being uniform in each stream in accord with the experimentally-determined values [9]. The co-flow boundary (r=20D) is treated as a perfect-slip wall. Symmetry conditions are applied on the centerline (r=0). At the exit plane, in the FV part, the mean density and the axial and radial mean velocities are extrapolated from the interior, and the pressure is specified.

Systematic tests have been performed on the following numerical parameters to determine appropriate values used in the current calculations: (i) the ISAT (In-Situ-Adaptive Tabulation) [21] error tolerance (2×10^{-5}), (ii) the number of cells in the domain (96×96), (iii) the number of particles per cell (100), and (iv) the coefficients of time averaging (over 1000 particle time steps). These values ensure that numerical errors are no greater than 2% (with respect to the peak value) for the mean temperature and major species, and 5% for the minor species.

4. Results and discussion

It has been shown in previous studies that both radiation and the pilot temperature T_p can significantly affect the calculations of flame F [2,22]. In the current work, the effect of T_p has been tested using the skeletal mechanism and the effect of radiation has been tested using the skeletal and GRI3.0 mechanisms. For more details refer to [6]. All of the calculations presented in this paper are obtained using the pilot temperature T_p =1880K and without radiation.

4.1 Calculations of the velocity field and the mixture fraction

Correct representation of the velocity field and mixture fraction is essential for the calculations of turbulent reactive flows. The radial profiles of the mean and rms axial velocities obtained using the S5G211, Smooke and GRI3.0 mechanisms with C_φ=2.0, together with the calculations using GRI3.0 mechanism with C_φ=1.5, are shown in Fig.1. Although there are some differences between these calculations (especially calculations using the Smooke mechanism), they are generally very close to each other, and agree with the experimental data reasonably well. Calculations using other mechanisms (i.e., ARM2, skeletal, and GRI211) yield similar velocity profiles (not shown) as Fig. 1.

Figure 2 shows the radial profiles of the mean and rms mixture fraction obtained using the skeletal, Smooke and GRI3.0 mechanisms with C_φ=2.0, together with the calculations using the GRI3.0 mechanism with C_φ=1.5. It can be seen that while the mean radial profiles of mixture fraction are almost identical for all these calculations shown in Fig. 2, the rms of mixture fraction has some obvious differences between the different mechanisms. For the GRI3.0 mechanism, calculations using a smaller value of C_φ (1.5) yield higher values of the rms of the mixture fraction, which is as expected. The same observations can be made for other calculations using other mechanisms (S5G211, ARM2, and GRI2.11, not shown).

4.2 Calculations of the conditional mean and rms

The conditional mean and rms of all species in flame F at z/D=1, 2, 3, 7.5, 15, 30, 45, 60, and 75 are calculated in the current work. It is found that that the conditional mean and rms are very sensitive to different mechanisms and different values of C_φ at z/D=7.5, 15, and 30, where significant local extinction and reignition are observed [1,4,9], but not so sensitive at other locations. Especially, the conditional means of the temperature and major species are almost identical at the downstream locations (z/D=45, 60, and 75). Significant differences can be observed in some minor species like CO and NO. To illustrate this point, Figure 3 shows the conditional mean temperature obtained using the S5G211 and GRI3.0 mechanisms, which are the most simple mechanism and most comprehensive mechanism used in the current work, respectively.

It can be seen from Fig. 3 that the conditional mean temperatures of all three calculations are very close to each other and agree very well with the experimental data at z/D=1, 2, 3, 45, 60 and 75, although there are small discrepancies between calculations using the GRI3.0 and S5G211 mechanisms at z/D=1, 2 and 3. On the other hand, these calculation are very different at z/D=7.5, 15, and 30. Among these locations, z/D=15 has the most significant local extinction and hence is most sensitive to different mechanisms and different values of C_φ. A similar tendency has been observed for other calculations (not shown).

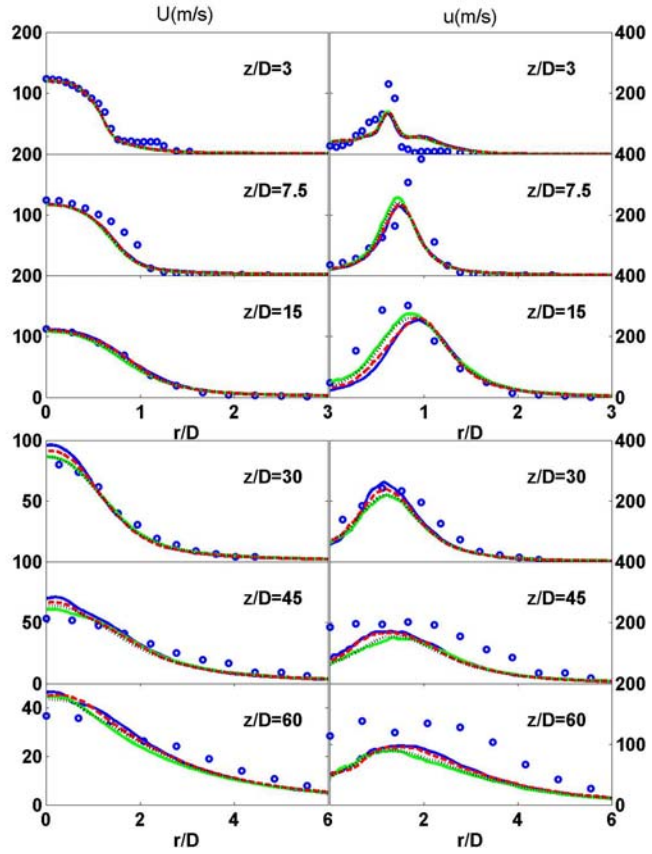

Fig. 1. *Computed and measured radial profiles of mean and rms axial velocity. Symbols, measurements [20]; lines, PDF calculations using: the S5G211 mechanism with C_φ=2.0 (blue solid), the Smooke mechanism with C_φ=2.0 (green solid), the GRI3.0 mechanism with C_φ=2.0 (red dashed), and the GRI3.0 mechanism with C_φ=1.5 (black dotted).*

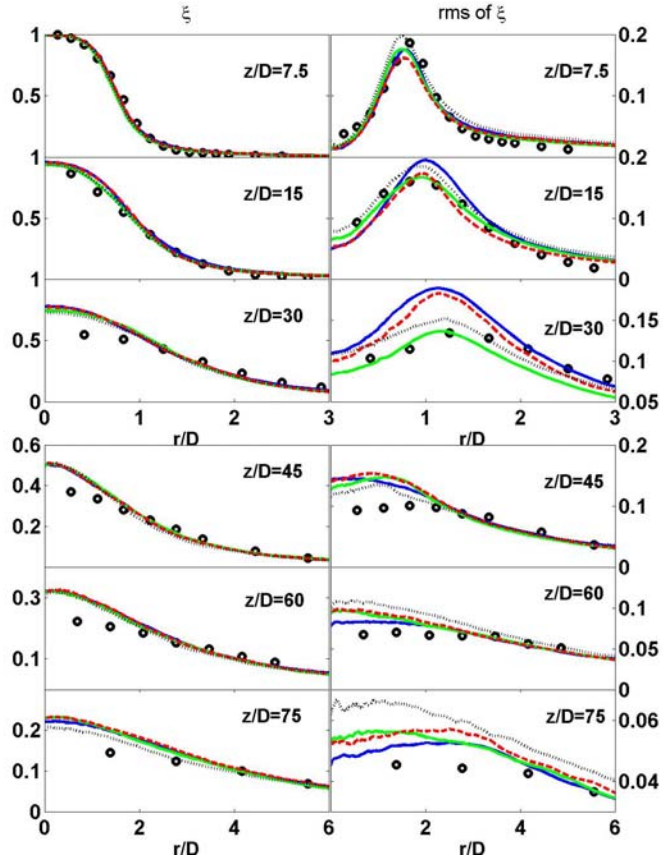

Fig. 2. *Computed and measured radial profiles of mean and rms mixture fraction. Symbols, measurements [9]; lines, PDF calculations using: the skeletal mechanism with C_φ=2.0 (blue solid), the Smooke mechanism with C_φ=2.0 (green solid), the GRI3.0 mechanism with C_φ=2.0 (red dashed), and the GRI3.0 mechanism with C_φ=1.5 (black dotted).*

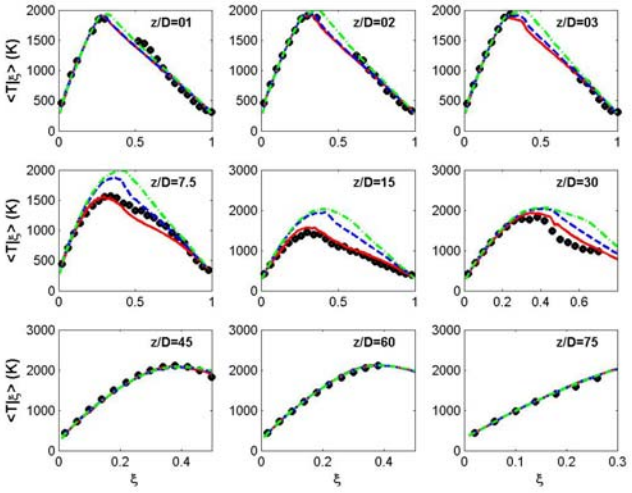

Fig. 3. *Measured and computed conditional mean temperature. Symbols, measurements [9]; lines, PDF calculations using: the S5G211 mechanism with C_φ=2.0 (green dash dotted), the GRI3.0 mechanism with C_φ=2.0 (blue dashed), and the GRI3.0 mechanism with C_φ=1.5 (red solid).*

4.3 Comparison of different mechanisms

Since the calculations are very sensitive to the mechanisms and the value of C_φ at z/D=15, it is natural to chose this location to investigate the performances of different mechanisms. The temperature, one characteristic major species (CH_4) and one characteristic minor species (CO) are studied at this location. Six mechanisms and four values of C_φ have been used for these calculations, as listed in Table 3 and the results are shown in Figs. 4 and 5.

Several observations can be made based on Figs. 4 and 5. First, for all mechanisms, the conditional rms decreases with increasing C_φ, which is as expected. In Fig. 4, for the skeletal, ARM2 and S5G211 mechanisms, the differences between the calculations obtained using smaller values of C_φ (e.g., 1.5 and 2.0) are much larger than those obtained using larger values of C_φ (e.g., 2.0 and 3.0). This indicates that these calculations become more and more sensitive to the change of the mixing rate as the calculations get closer to global extinction. Second, in the current test cases, each

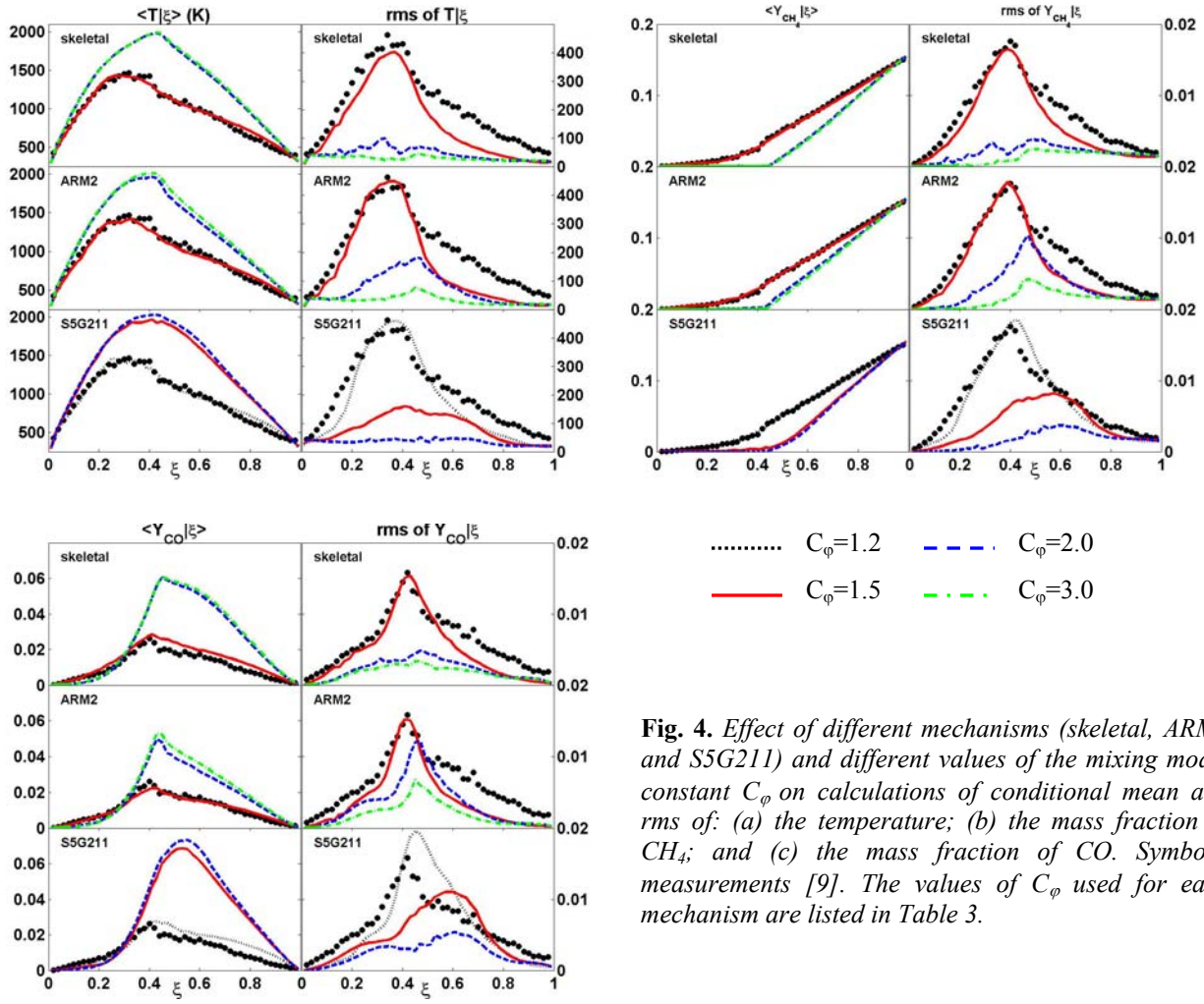

Fig. 4. *Effect of different mechanisms (skeletal, ARM2 and S5G211) and different values of the mixing model constant C_φ on calculations of conditional mean and rms of: (a) the temperature; (b) the mass fraction of CH_4; and (c) the mass fraction of CO. Symbols, measurements [9]. The values of C_φ used for each mechanism are listed in Table 3.*

Table 3. List of mechanisms and the values of C_φ used in current work (* denotes the case that yield the closest agreement with the measurements for tested values of C_φ)

Mechanisms	C_φ				Shown in
	1.2	1.5	2.0	3.0	
Skeletal		Yes*	Yes	Yes	Fig. 4
ARM2		Yes*	Yes	Yes	Fig. 4
S5G211	Yes*	Yes	Yes		Fig. 4
GRI 2.11		Yes*	Yes		Fig. 5
GRI 3.0		Yes*	Yes		Fig. 5
Smooke			Yes*	Yes	Fig. 5

mechanism has a value of C_φ (which is marked by "*" in Table 3, and denoted as C_φ^* in the following) that yields closest agreement with the measurements. In other words, all of these mechanisms are capable of representing the local extinction of flame F by using appropriate values of C_φ. Based on test cases in the current work, these values are: C_φ^*=1.5 for the ARM2, GRI2.11, GRI3.0 and skeletal mechanisms; C_φ^*=1.2 for the S5G211 mechanism and C_φ^*=2.0 for the Smooke mechanism. It should be noted that, because discrete values of C_φ are used in the current work, there might exist different values of C_φ^* that could yield even better agreement with the experimental data. For example, the calculations using GRI2.11 with C_φ^* =1.5 over-predict the measured conditional mean temperature a little bit, which indicates that calculations using a smaller value of C_φ (e.g., 1.4) may be even closer to the measurements. Third, the closest agreement with a conditional mean corresponds to closest agreement with its conditional rms. For these closest-agreement calculations, they agree reasonably well with the measured conditional rms's around stoichiometric (ξ_{st}=0.351) and on the lean side. They generally under-represent the rms's on the fuel rich side.

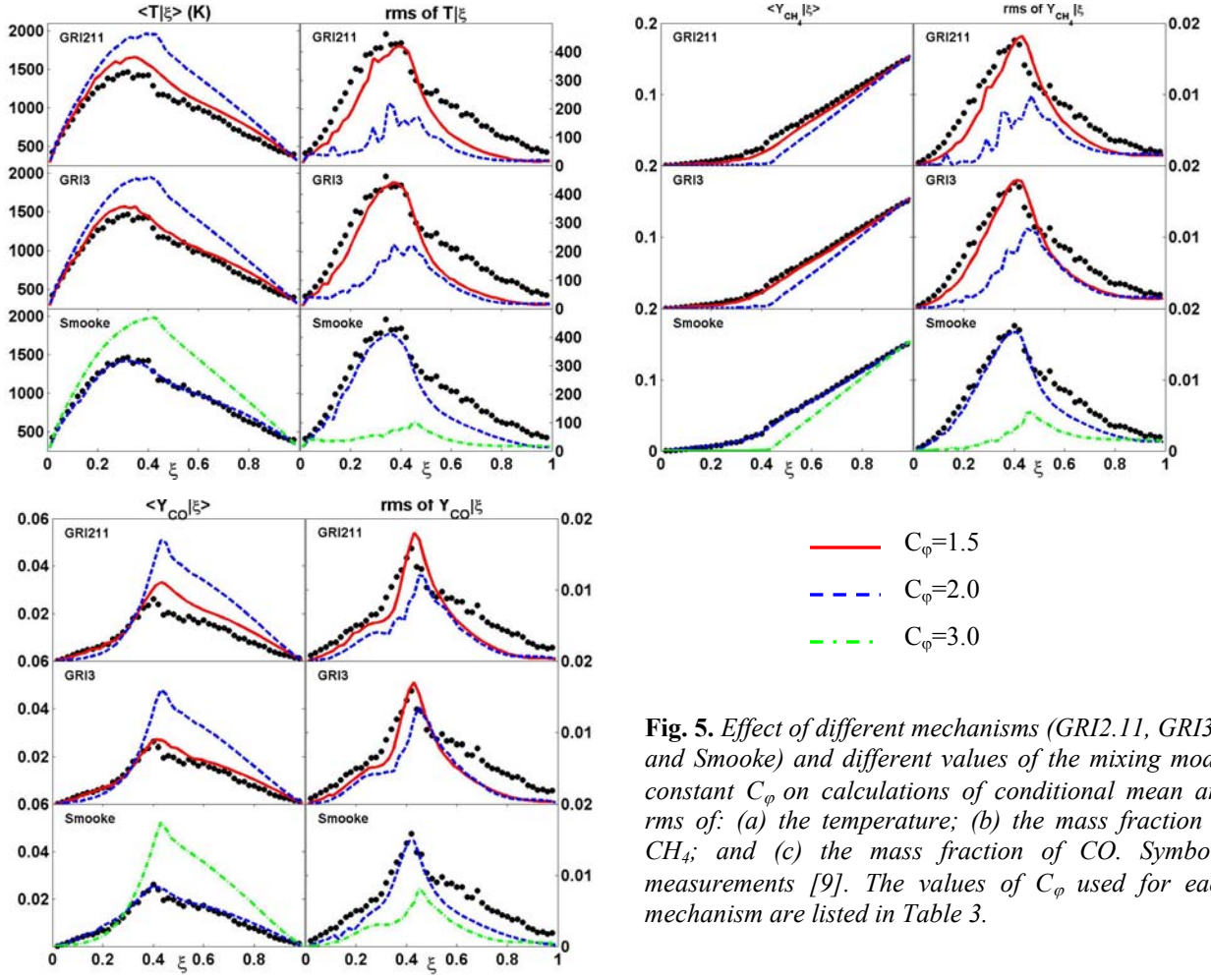

Fig. 5. *Effect of different mechanisms (GRI2.11, GRI3.0 and Smooke) and different values of the mixing model constant C_φ on calculations of conditional mean and rms of: (a) the temperature; (b) the mass fraction of CH_4; and (c) the mass fraction of CO. Symbols, measurements [9]. The values of C_φ used for each mechanism are listed in Table 3.*

4.4 Performance of GRI mechanisms and calculations of the NO

It has been shown in previous studies [23] that calculations of laminar opposed-flow partially premixed methane/air flames using ARM2, GRI2.11 and GRI3.0 yield similar results for major species, while there may be significant differences for minor species. The current calculations indicate a similar tendency. While all of these three mechanisms yield closest agreement with the experimental data with C_φ^*=1.5, the S5G211 calculations have different behavior and obtain closest agreement with C_φ^*=1.2.

Figure 6 shows the mass fraction of NO conditional on mixture fraction at different axial locations for ARM2, GRI2.11, GRI3.0 and S5G211, all with their closest-agreement cases. It may be seen that the calculations using GRI3.0 yield significantly higher levels of NO than those obtained using the ARM2 and GRI2.11 mechanisms. The ARM2 calculations and GRI2.11 calculations have some differences at z/D=15, but they are very close to each other at other locations. This is consistent with the laminar flame

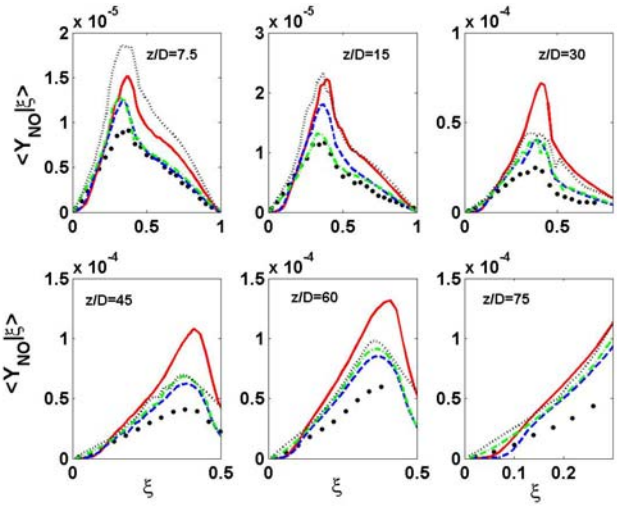

Fig. 6. *Comparisons of different GRI mechanisms in their closest-agreement cases using the conditional mean mass fraction of NO in flame F. Symbols, measurements [9]; lines, PDF calculations using the GRI3.0 mechanism (red solid line), the GRI2.11 mechanism (blue dashed line), the ARM2 mechanism (green dash dotted line) and S5G211 mechanism (black dotted line). The EMST mixing model is used for all of these calculations with C_φ=1.5 (except C_φ=1.2 for the S5G211 mechanism).*

studies performed by Barlow et al. [23] and the composition PDF calculations of flame D performed by Raman et al. [24]. The calculations using the S5G211 mechanism yield significantly higher levels of NO at z/D=7.5 and 15, but yield the same level as that of ARM2 and GRI2.11 at other locations. It should be noticed that all the calculations presented in the current paper are obtained without considering the effect of radiation. Since radiation has a significant effect on the mass fraction of NO, the agreement with the experimental data will change when radiation is taken into consideration. Presumably, the observations about the relative tendency will still be valid.

5. Conclusions

In the current work, joint PDF calculations with six different chemistry mechanisms (i.e., ARM2, GRI2.11, GRI3.0, S5G211, skeletal, and Smooke) have been performed on Flame F. This flame is well known to have significant local extinction and exhibits the strongest sensitivity. Hence it is very useful for investigating the performance of different chemistry mechanisms, especially the capability to capture location extinction and reignition.

The EMST mixing model with a series values of mixing model constant C_φ is used for these calculations. It is found that all six mechanisms are capable of capturing the local extinction by using appropriate values of C_φ. While calculations using the ARM2, GRI2.11, GRI3.0 and skeletal mechanisms with C_φ=1.5 yield closest agreement with the experimental data, the S5G211 and Smooke calculations behavior differently and yield closest agreement with the experimental data by using C_φ=1.2 and 2.0, respectively.

The calculations using the GRI3.0 mechanism generally yield significantly higher levels of NO in flame F than those of ARM2 and GRI2.11 mechanisms. The calculations using the S5G211 mechanism yield higher levels of NO at z/D=7.5 and z/D 15 than those of ARM2 and GRI2.11, but almost the same level at z/D=30 and after.

Acknowledgements

This work is supported by Air Force Office of Scientific Research under grant No. F-49620-00-1-0171. The computations were conducted using the resources of the Cornell Theory Center, which receives funding from Cornell University, New York State, federal agencies, foundations, and corporate partners.

References:

1. Xu, J. and S.B., Pope, Combust. Flame, 123 (2000) 281-307
2. Tang, Q., J. Xu and S.B. Pope , Proc. Combust. Inst., 28 (2000) 133-139
3. Lindstedt, R. P., S.A. Louloudi and E.M. Vaos, Proc. Combust. Inst, 28 (2000) 149-156
4. Barlow, R. S. and J. H., Frank, Proc. Combust. Inst, 27 (1998) 1087-1095
5. Ren, Z. and S.B. Pope, Combust. Flame, 136 (2004) 208-216
6. Cao, R., S.B. Pope, and A.R. Masri, "Turbulent Lifted Flames in a Vitiated Coflow Investigated Using Joint PDF Calculations", Combust. Flame, accepted, 2005
7. Mallampalli, H. P., T. H., Fletcher and J.Y. Chen, Paper 96F-098, Presented at the Fall Meeting of the Western States Section of the Combustion Institute University of Southern California, Los Angeles, CA October 28-29, 1996
8. GRI-Mech Web site, http://www.me.berkeley.edu/gri-mech
9. Web site for the International Workshop on Measurement and Computaion of Turbulent Nonpremixed Flames (TNF), R. S. Barlow, Ed., Sandia National Laboratories, http://www.ca.sandia.gov/tdf/Workshop.
10. Cao, R. and S.B. Pope, Combust. Flame, The Influence of Chemical Mechanisms on PDF calculations of Nonpremixed Piloted Jet Flames, (in preparation), 2005
11. Pope, S.B., Prog. Energy Combust. Sci., 11 (1985) 119-192
12. Van Slooten, P.R., Jayesh and S.B. Pope, Phys. Fluids, 10 (1998) 246-265
13. Jenny, P., M. Muradoglu, K. Liu, S. B. Pope and D. A. Caughey, J. Comput. Phys., 169 (2001) 1-23
14. Muradoglu, M., S.B. Pope and D.A. Caughey, J. Comp. Phys., 172 (2001) 841-878
15. Subramaniam, S. and S.B. Pope, Combust. Flame, 115 (1998) 487-514
16. Sung, C.J., C.K. Law and J.Y. Chen, Proc. Combust. Inst., 27 (1998) 295-304
17. James, S., M.S., Anand, M.K., Razdan and S.B., Pope, in Proceeding of ASME Turbo Expo Land, Sea & Air 1999, The Forty-Fourth ASME Gas Turbine and AeroEngine Technical Congress, Indianapolis, IN,
18. Smooke, M.D., I.K., Puri and K., Seshadri, Proc. Combust. Inst., 21, (1986) 1783-1792.
19. Bennett B.A.V. and M.D., Smooke, (private communication).
20. Schneider, Ch., A. Dreizler, J. Janicka and E.P. Hassel, Combust.Flame, 135, (2003) 185-190
21. Pope, S.B., Combust. Theory Modelling, 1 (1997) 41-63
22. Tang, Q., Ph.D. Thesis, Cornell University, 2003
23. Barlow, R.S., A.N. Karpetis, J.H. Frank and J.Y. Chen, Combust. Flame 127 (2001) 2102-2118
24. Raman, V., R.O. Fox and A.D. Harvey, Combust. Flame, 136, (2004) 327-350